Landes Bioscience www.landesbioscience.com

Supplemental Material to:

Kumsal Ayse Tekirdag, Gozde Korkmaz, Deniz Gulfem Ozturk, Reuven Agami and Devrim Gozuacik

MIR181A regulates starvation- and rapamycin-induced autophagy through targeting of ATG5

Autophagy 2012; 9(3)
http://dx.doi.org/10.4161/auto.23117

www.landesbioscience.com/journals/autophagy/article/23117

Suppl.Fig.1

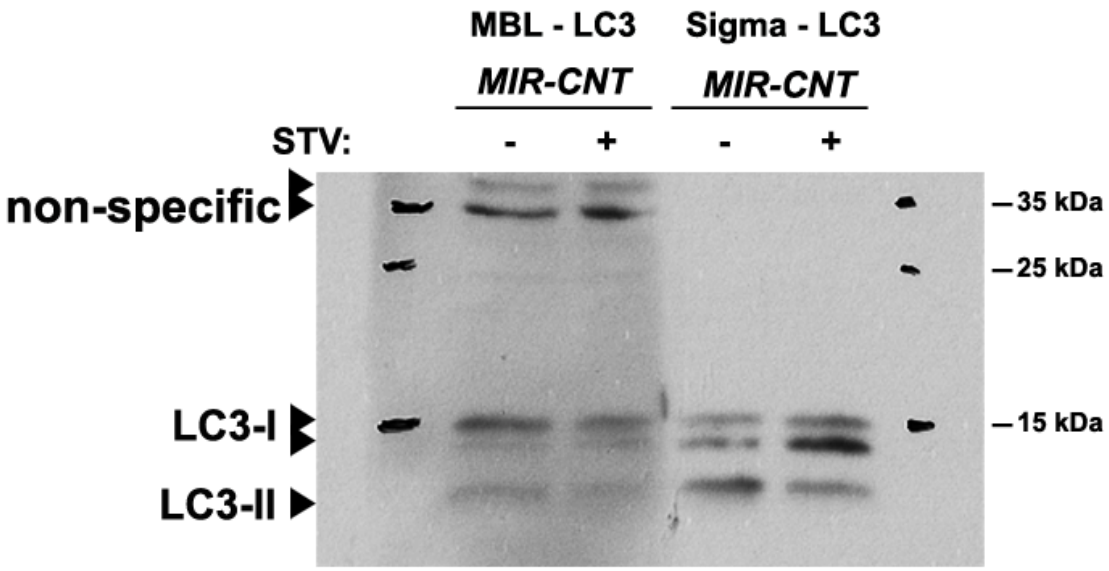
MBL - LC3
Sigma - LC3
MIR-CNT
MIR-CNT
STV:
-
+
-
+
non-specific
LC3-I
LC3-II
35 kDa
25 kDa
15 kDa

Suppl. Fig.2

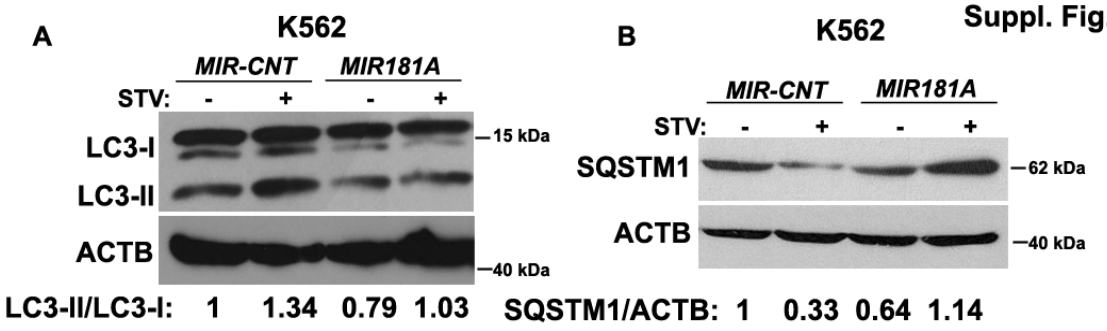
A
K562
MIR-CNT
MIR181A
STV: - + - +
LC3-I
LC3-II
ACTB
15 kDa
40 kDa
LC3-II/LC3-I: 1 1.34 0.79 1.03
B
K562
MIR-CNT
MIR181A
STV: - + - +
SQSTM1
ACTB
62 kDa
40 kDa
SQSTM1/ACTB: 1 0.33 0.64 1.14

Suppl. Fig.3

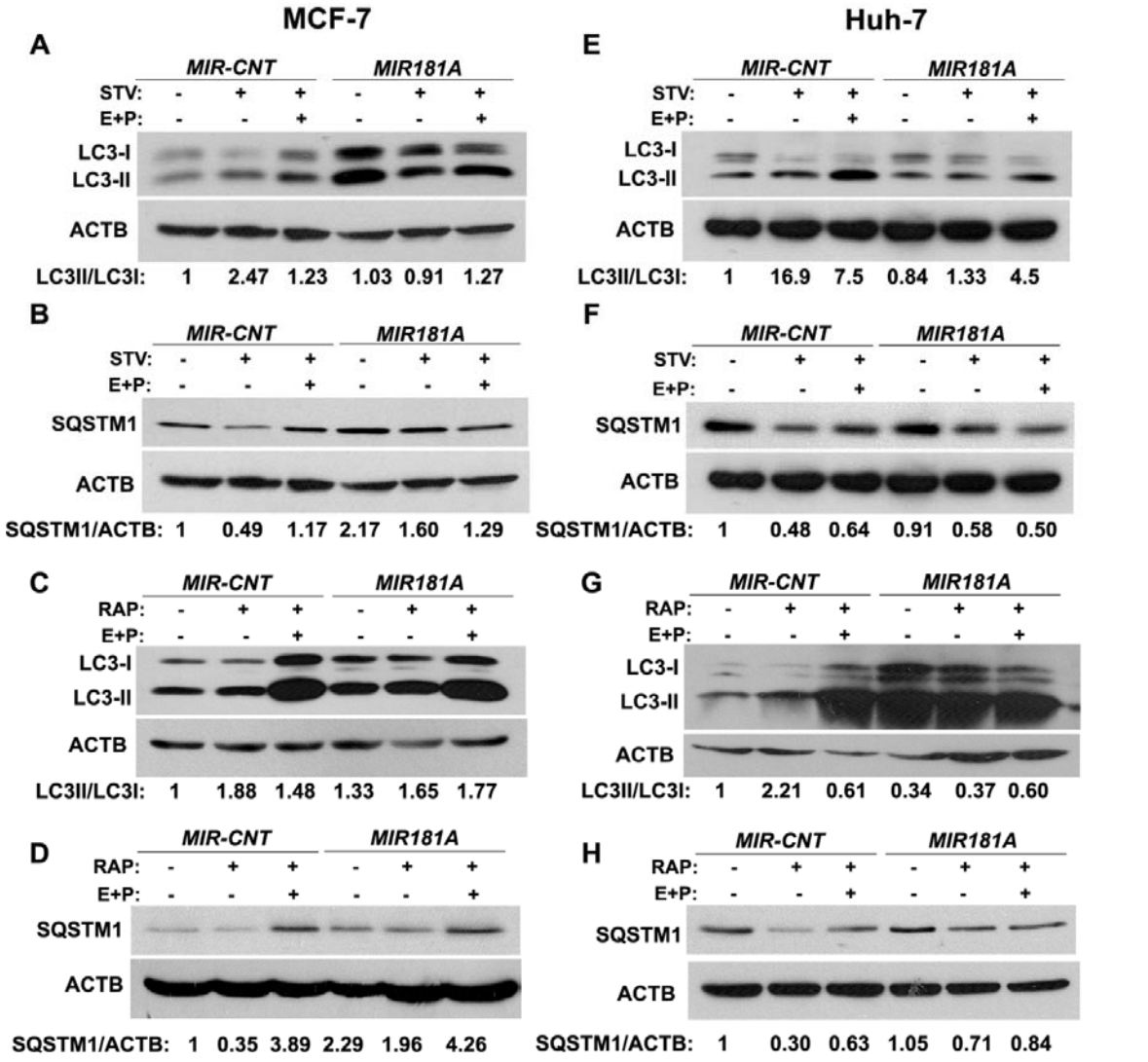
MCF-7
Huh-7
A
E
MIR-CNT
MIR181A
STV:
E+P:
LC3-I
LC3-II
ACTB
LC3II/LC3I: 1 2.47 1.23 1.03 0.91 1.27
LC3II/LC3I: 1 16.9 7.5 0.84 1.33 4.5
B
F
SQSTM1
SQSTM1/ACTB: 1 0.49 1.17 2.17 1.60 1.29
SQSTM1/ACTB: 1 0.48 0.64 0.91 0.58 0.50
C
G
RAP:
LC3II/LC3I: 1 1.88 1.48 1.33 1.65 1.77
LC3II/LC3I: 1 2.21 0.61 0.34 0.37 0.60
D
H
SQSTM1/ACTB: 1 0.35 3.89 2.29 1.96 4.26
SQSTM1/ACTB: 1 0.30 0.63 1.05 0.71 0.84

Suppl.Fig.4

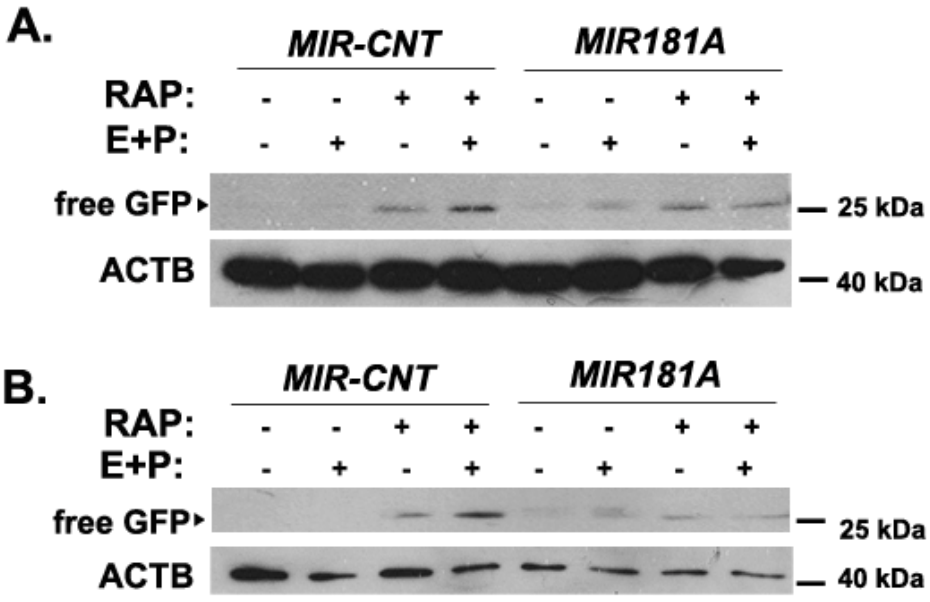
A.
MIR-CNT
MIR181A
RAP:
E+P:
free GFP
ACTB
25 kDa
40 kDa
B.
MIR-CNT
MIR181A
RAP:
E+P:
free GFP
ACTB
25 kDa
40 kDa

Suppl.Fig.5

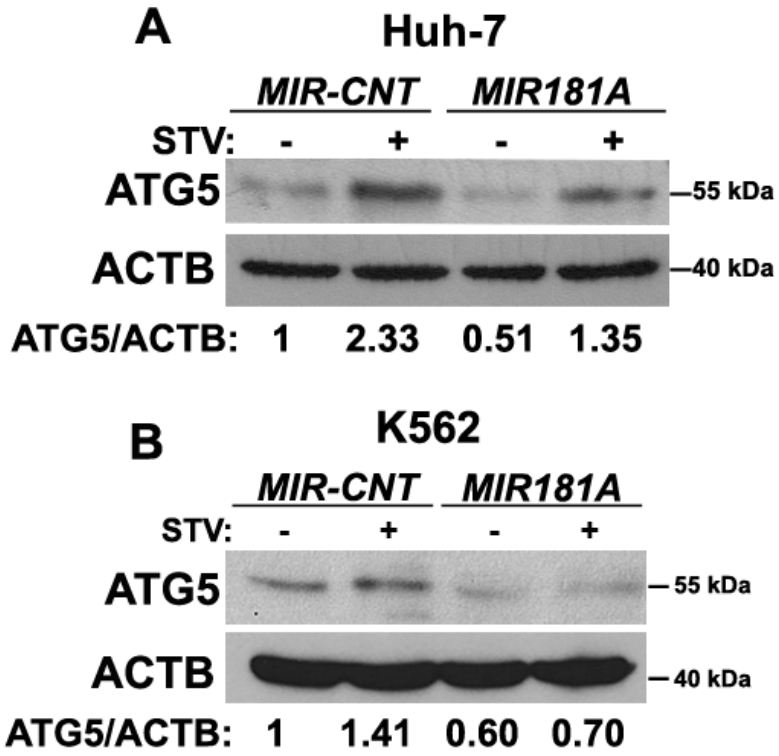
A
Huh-7
MIR-CNT
MIR181A
STV: - + - +
ATG5
55 kDa
ACTB
40 kDa
ATG5/ACTB: 1 2.33 0.51 1.35
B
K562
MIR-CNT
MIR181A
STV: - + - +
ATG5
55 kDa
ACTB
40 kDa
ATG5/ACTB: 1 1.41 0.60 0.70

Suppl. Fig.6

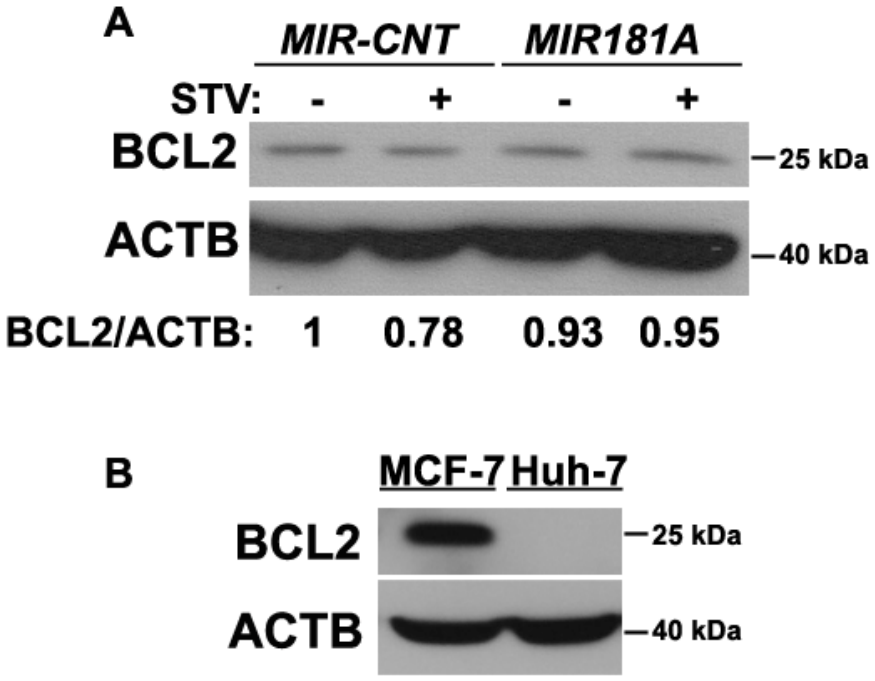
A
MIR-CNT
MIR181A
STV: - + - +
BCL2
25 kDa
ACTB
40 kDa
BCL2/ACTB: 1 0.78 0.93 0.95
B
MCF-7
Huh-7
BCL2
25 kDa
ACTB
40 kDa

Suppl. Fig.7

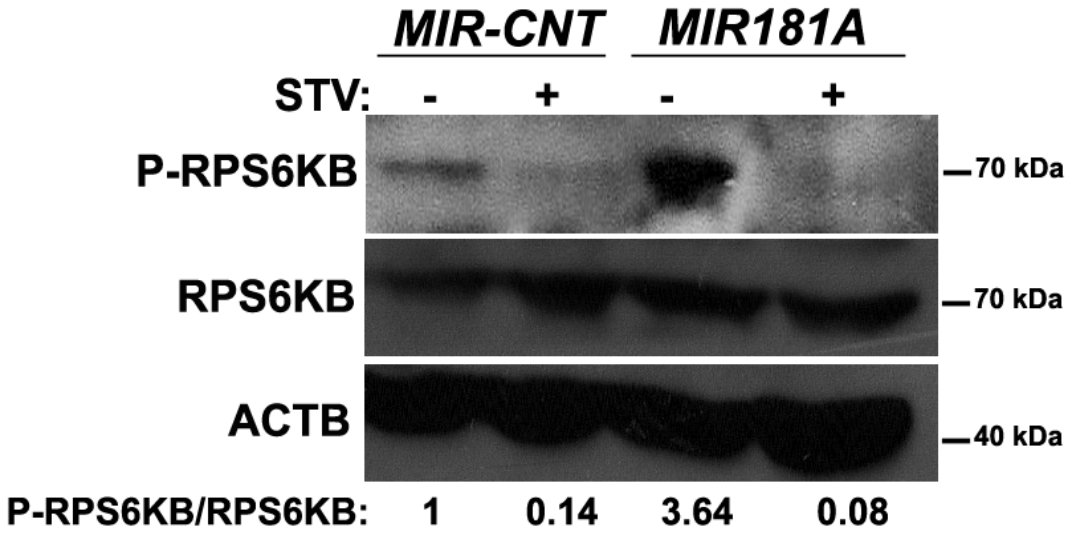
MIR-CNT
MIR181A
STV: - + - +
P-RPS6KB
70 kDa
RPS6KB
70 kDa
ACTB
40 kDa
P-RPS6KB/RPS6KB: 1 0.14 3.64 0.08

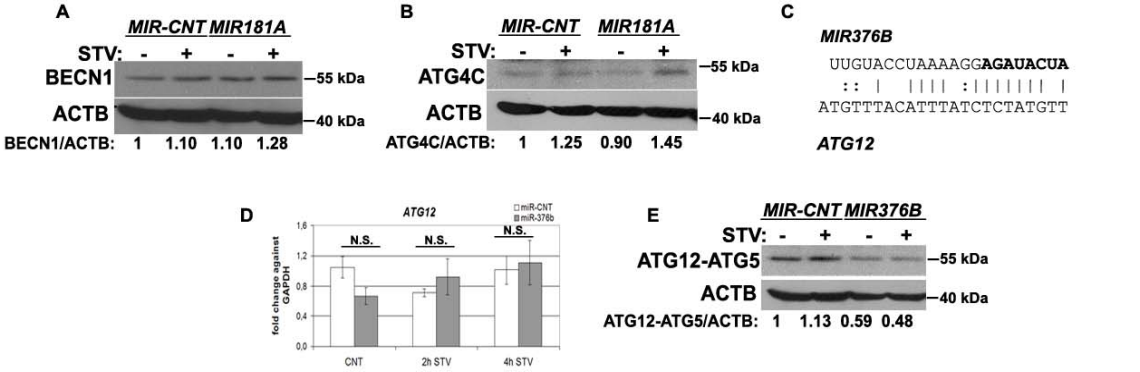
A
MIR-CNT MIR181A
STV: - + - +
BECN1
ACTB
55 kDa
40 kDa
BECN1/ACTB: 1 1.10 1.10 1.28
B
MIR-CNT MIR181A
STV: - + - +
ATG4C
ACTB
55 kDa
40 kDa
ATG4C/ACTB: 1 1.25 0.90 1.45
C
MIR376B
UUGUACCUAAAAGGAGAUACUA
ATGTTTACATTTATCTCTATGTT
ATG12
D
ATG12
miR-CNT
miR-376b
fold change against GAPDH
N.S.
N.S.
N.S.
CNT
2h STV
4h STV
E
MIR-CNT MIR376B
STV: - + - +
ATG12-ATG5
ACTB
55 kDa
40 kDa
ATG12-ATG5/ACTB: 1 1.13 0.59 0.48

Supplementary Fig.9

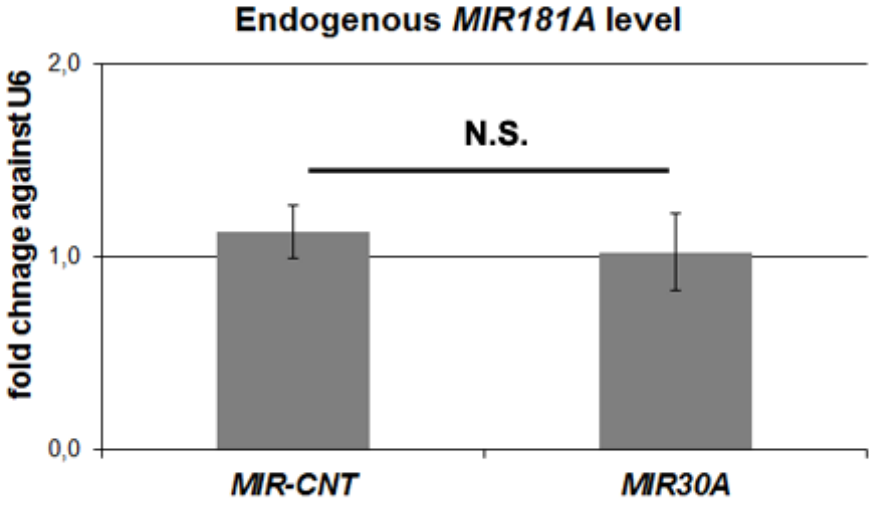

Suppl.Fig.10

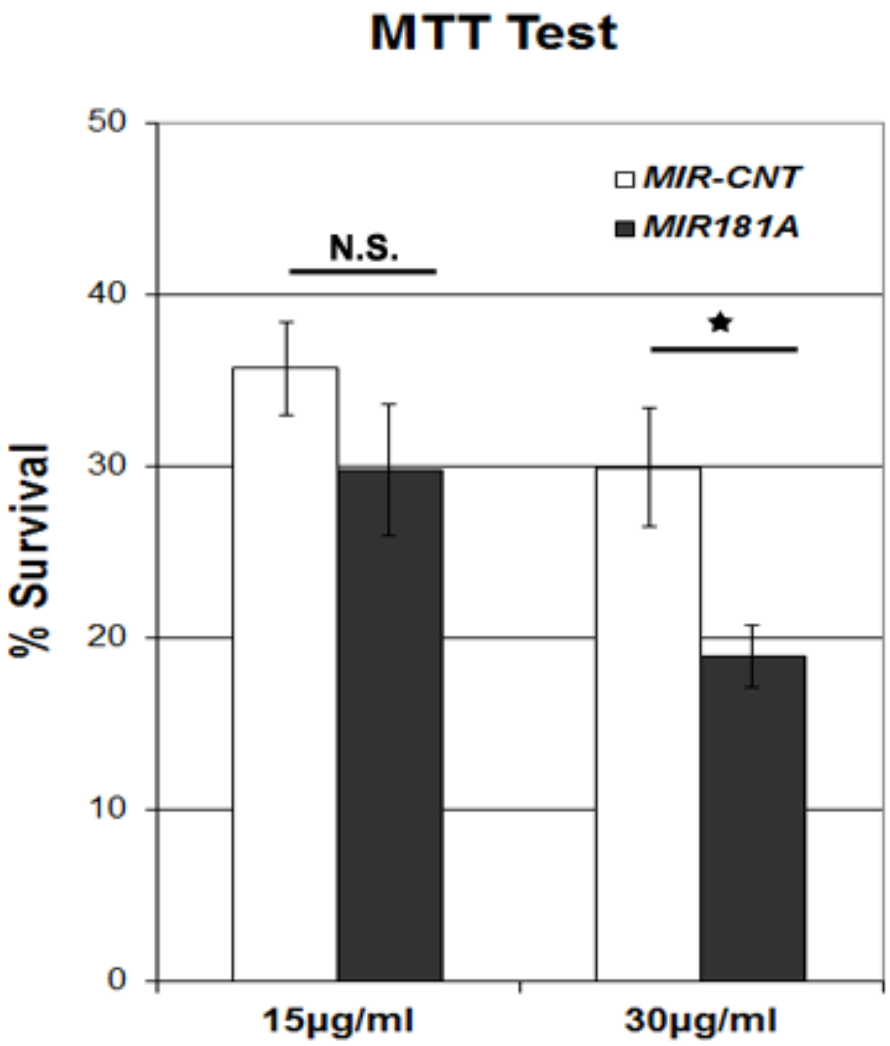
MTT Test
% Survival
50
40
30
20
10
0
MIR-CNT
MIR181A
N.S.
★
15µg/ml
30µg/ml

Supplementary Figure Legends

Supplementary Figure 1. LC3-I migrated as a double band. Cell extracts from the same experiment were loaded twice in parallel wells, run on the same gel and blotted together. The membrane was divided into two for incubation with anti-LC3B antibody of MBL (PM036) or Sigma (L7543). Double arrowhead indicates LC3-I bands.

Supplementary Figure 2. Effect of *MIR181A* on autophagy is not cell type-dependent. **(**A) *MIR181A* blocked starvation-induced LC3-I to LC3-II conversion in K562 cells. LC3-II/LC3-I ratios were calculated using ImageJ densitometric analysis. (D) *MIR181A* blocked starvation-induced SQSTM1 degradation in K562 cells. SQSTM1/ACTB ratios were calculated.

Supplementary Figure 3. Overexpression of *MIR181A* resulted in decreased autophagic activity in MCF-7 and Huh-7 cells. Tests were performed in the presence or absence of E64d (10 μg/ml) and pepstatin A (10 μg/ml) (E+P). (A and E) *MIR181A* decreased starvation-induced conversion of LC3-I to LC3-II in MCF-7 and Huh-7 cells, respectively. Immunoblot results of extracts from non-starved (STV-) or starved (STV+) cells. LC3-II/LC3-I densitometric ratios were marked. ACTB was used as a loading control. (B and F) *MIR181A* blocked starvation induced SQSTM1 degradation in MCF-7 and Huh-7 cells, respectively. ACTB was used as a loading control. SQSTM1/ACTB densitometric ratios were marked. (C and G) *MIR181A* decreased LC3-I to LC3-II conversion stimulated by rapamycin (RAP) in MCF-7 and Huh-7 cells. LC3-II/LC3-I ratios were marked. (D and H) *MIR181A* blocked rapamycin induced SQSTM1 degradation in MCF-7 and Huh-7 cells.

Supplementary Figure 4. GFP-LC3 lysosomal delivery and proteolysis test. MCF-7 cells were transiently co-transfected with GFP-LC3 and *MIR-CNT* or *MIR181A* and treated with

carrier (DMSO) or rapamycin (2.5 nM, 24 h) in the presence or absence of E64d (10 μg/ml) and pepstatin A (10μg/ml) (E+P). Appearance of free GFP was analyzed in immunoblots. ACTB was used as a loading control. Results of two independent experiments were shown in A and B.

Supplementary Figure 5. Overexpression of *MIR181A* led to a decrease in ATG5 protein levels in Huh-7 and K562 cells**.** (A) *MIR181A* overexpression resulted in decreased ATG5 protein levels in Huh-7 cells. Immunoblots of control (*MIR-CNT*) or *MIR181A* transfected cells that were non-starved (STV-) or starved (STV+). ACTB was used as loading control. ATG5/ACTB band densitometric ratios were shown. (B) Similar decrease in ATG5 protein levels in K562 cells following *MIR181A* expression.

Supplementary Figure 6. Effect *MIR181A* overexpression on BCL2 protein levels in MCF-7 and Huh-7 cells. (A) BCL2 protein levels were not decreased following *MIR181A* expression in MCF-7 cells. Immunoblots of control (*MIR-CNT*) or *MIR181A* transfected and non-starved (STV-) or starved (STV+) cells. ACTB was used as loading control. BCL2/ACTB densitometric levels were shown. (B) Lack of BCL2 protein expression in Huh-7 cells. MCF-7 cell extract was used as positive control. ACTB was used as loading control.

Supplementary Figure 7. *MIR181A* overexpression could not overcome starvation-related MTOR inhibition. Immunoblot showing P-RPS6KB and total RPS6KB levels in non-starved (STV-) or starved (STV+) MCF-7 cell extracts. ACTB was used as loading control. P-RPS6KB /RPS6KB densitometric ratios were calculated.

Supplementary Figure 8. Other potential miRNA targets during autophagy. (A) BECN1 and (B) ATG4C protein levels were not responsive to *MIR181A* overexpression in MCF-7 cells. (C) *MIR376B* target sequence in the 3'UTR of *ATG12* mRNA predicted by bioinformatics

analyses. Bold sequences, *MIR376B* seed sequences. (D) Quantitative PCR (qPCR) analysis of *ATG12* (GenBank accession number: NM_004707.2, 382-405) mRNA levels in control (*MIR-CNT*) or *MIR376B* transfected (*MIR-376B*) and non-starved (CNT) or starved (STV) MCF-7 cells. Data were normalized using *GAPDH* mRNA levels. (E) ATG12–ATG5 protein complex levels were decreased following *MIR376B* expression in MCF-7 cells. Immunoblots of *MIRCNT* or *MIR376B* transfected cells that were non-starved (STV-) or starved (STV+). ACTB was used as loading control. ATG5-specific antibody was used to reveal the complex. ATG12–ATG5 complex/ACTB band densitometric ratios were shown.

Supplementary Figure 9. TaqMan quantitative PCR (qPCR) analysis of endogenous *MIR181A* levels in control (*MIR-CNT*) or *MIR30A* overexpressing cells. Endogenous *MIR181A* levels were not significantly altered following *MIR30A* overexpression (mean ± S.D. of independent experiments, n=6, N.S., not significant). qPCR data were normalized using *U6 small nuclear 1 (RNU6-1) (U6)* mRNA levels.

Supplementary Figure 10. *MIR181A* potentiated chemotherapy-induced toxicity of cisplatin in MCF-7 breast cancer cells. Quantification of cisplatin-induced (24 h, 15 μg/ml or 30 μg/ml) cell death using MTT test. % survival was calculated by normalizing experimental values to the survival of DMSO (carrier)-treated cells (mean ± SD of independent experiments, n = 4, *$p < 0.05$. N.S., not significant).